Available online at www.sciencedirect.com
ScienceDirect
Journal of Solid State Chemistry 180 (2007) 467–473
JOURNAL OF SOLID STATE CHEMISTRY
www.elsevier.com/locate/jssc

Energy transfer and heat-treatment effect of photoluminescence in Eu^{3+}-doped $TbPO_4$ nanowires

Weihua Di[a,*], Xiaojun Wang[a], Peifeng Zhu[a], Baojiu Chen[b]

[a]*Key Laboratory of Excited State Processes, Changchun Institute of Optics, Fine Mechanics and Physics, Chinese Academy of Sciences, Changchun 130033, People's Republic of China*
[b]*Department of Physics, Dalian Maritime University, Dalian 116026, People's Republic of China*

Received 28 August 2006; received in revised form 30 October 2006; accepted 4 November 2006
Available online 14 November 2006

Abstract

We have successfully synthesized Eu^{3+}-doped $TbPO_4$ nanowires, which are orderly organized to form bundle-like structure. A thermal treatment up to 600 °C does not modify the size, shape and structure of as-synthesized sample. Due to the energy overlap between Tb^{3+} and Eu^{3+}, an efficient energy transfer occurs from Tb^{3+} to Eu^{3+}. The effects of Eu^{3+} concentration and thermal treatment on the luminescent properties of Eu^{3+} are investigated. The increase of Eu^{3+} concentration leads to the increase of the energy transfer efficiency from Tb^{3+} to Eu^{3+}, but also enhances the probability of the interaction between neighboring Eu^{3+}, which results in the concentration quenching. With the heat-treatment, the luminescence of Eu^{3+} presents an obvious increase, but almost no change for the luminescence of Tb^{3+}. This difference is explained based on the TGA, DTA, and fluorescent decay dynamics analyses.

Keywords: Hydrothermal synthesis; Thermal effect; Rare earth; Energy transfer; Luminescence

1. Introduction

Nowadays, inorganic luminescent materials with nanometer dimensions have become an important field of modern nanoscale science and technology, which could find numerous potential applications in the fields of physics, chemistry and biology [1,2]. In particular, one-dimensional (1D) luminescent nanostructures have attracted considerable attention due to their potential applications as interconnectors and active components in fabricating the optoelectronic devices [3,4].

Rare earth compounds have been widely used in high-performance luminescent devices, magnets, catalysts, and other functional materials owing to the numerous well-defined transition modes involving the 4*f* shell of their ions [5]. Recently, more and more interest has been focused on the synthesis and photoluminescence of rare earth orthophosphates with nanosized scale for their potential application in optoelectronic devices and biological fluorescence labeling [6].

The aqueous synthesis including sol–gel, precipitation and hydrothermal method is commonly used to prepare the rare earth compound materials with nanosized scale [7,8]. The aqueous synthesis route may provide several adjustable synthetic parameters such as solution pH and concentration, and reaction time and temperature, thus the size, shape, morphology, and structure can be effectively controlled [9,10]. Several research groups used the hydrothermal method to synthesize rare earth compounds with different shapes and structures by changing the solution pH and the reaction temperature [11]. Jia et al. have successfully synthesized $LaVO_4$ nanocrystal with zircon-type structure using an ethylenediamine tetraacetic acid (EDTA)-assisted hydrothermal method [9]. This structure cannot be obtained by conventional solid-state reaction. Generally, the luminescent nanocrystal synthesized by low-temperature aqueous route shows low crystallinity, numerous structural defects, and a low luminescent efficiency [4,12]. The thermal treatment at a suitable temperature is an alternative strategy to improve the

*Corresponding author.
E-mail address: weihdi@yahoo.com.cn (W. Di).

0022-4596/$ - see front matter © 2006 Elsevier Inc. All rights reserved.
doi:10.1016/j.jssc.2006.11.006

crystallinity and luminescent efficiency [12]. In addition, the thermal treatment sometimes results in morphological variation, phase transition, and structural transformation [12,13]. These changes generally cause significant change of the materials' properties. In this work, we attempt to make the results on the energy transfer from Tb^{3+} to Eu^{3+} and the thermal treatment effects of photoluminescence of Tb^{3+} and Eu^{3+} in the nanosized samples. For this purpose, Eu^{3+}-doped $TbPO_4$ nanowires were synthesized by hydrothermal route. Energy transfer and heat-treatment effects of structure, morphology, and photoluminescence were investigated.

2. Experimental

Appropriate amounts of high purity Tb_4O_7 and Eu_2O_3 were dissolved in concentrated HNO_3 to form Tb(III) and Eu(III) solutions, respectively, to which, appropriate volume of $(NH_4)_2HPO_4$ solution was added slowly under vigorous stirring for 1 h. The final pH value was adjusted to 1–2 by the addition of aqueous ammonia (NH_4OH). The resulting suspension was pored into a Teflon-lined stainless steel autoclave. The autoclave was sealed and maintained at 100 °C for 12 h and then air-cooled to room temperature. The resulting products were filtered, washed with deionized water and absolute alcohol, and finally dried at 60 °C. A part of obtained powders were annealed at various temperatures ranging from 150 to 600 °C under N_2 atmosphere.

The crystal structure and morphology were obtained by X-ray diffraction (XRD) using a Cu target radiation resource ($\lambda = 1.54078$ Å) and scanning electron microscopy (SEM) utilizing a Hitachi S-4800 scanning electron microscope. Thermogravimetric analysis (TGA) of powders coupled with differential thermal analysis (DTA) was performed up to 600 °C at the heating rate of 10 °C/min under nitrogen gas flow (TA instruments, model SDT 2960, USA). The excitation spectrum and emission spectrum under 355-nm excitation were measured at room temperature with a Hitachi F-4500 fluorescence spectrometer. In the measurement of the fluorescent dynamics of Tb^{3+} and Eu^{3+}, a 355-nm light generated from a third-harmonic generator pumped by a pulsed Nd:YAG laser was used as the excitation source.

3. Results and discussion

Fig. 1 presents XRD patterns of the as-synthesized and heat-treated (600 °C) samples. It is noted that, for the as-synthesized sample, all the diffraction peaks could be well indexed to a hexagonal rhabdophane-type $TbPO_4$ hydrate (JCPDS No. 20–1244), and that no impurities are observed. Typical TGA and DTA plots of as-synthesized $TbPO_4$:$Eu \cdot nH_2O$ are given in Fig. 2(a) and (b). Two weight losses occur in two distinct steps with an overall weight loss of 7% from 40 to 600 °C. The first one occurs in the temperature range 60–140 °C, and is assigned to the release of residual water adsorbed at the powder surface due to the storage in air condition. Accordingly, it corresponds to a broad endothermic peak in the DTA

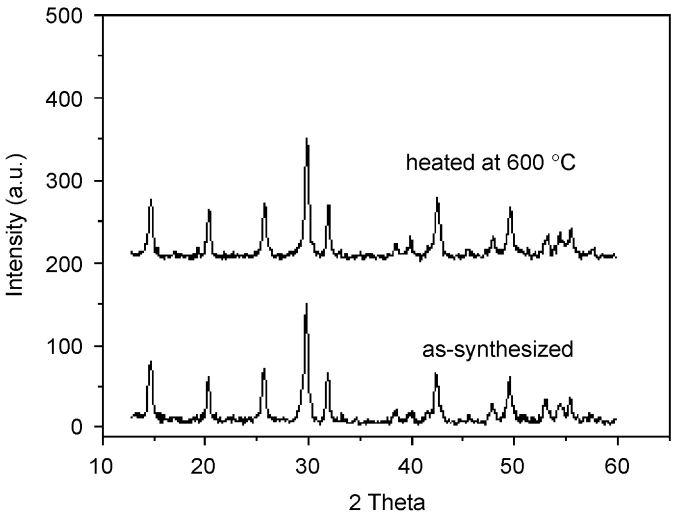

Fig. 1. XRD patterns of as-synthesized and heat-treated samples.

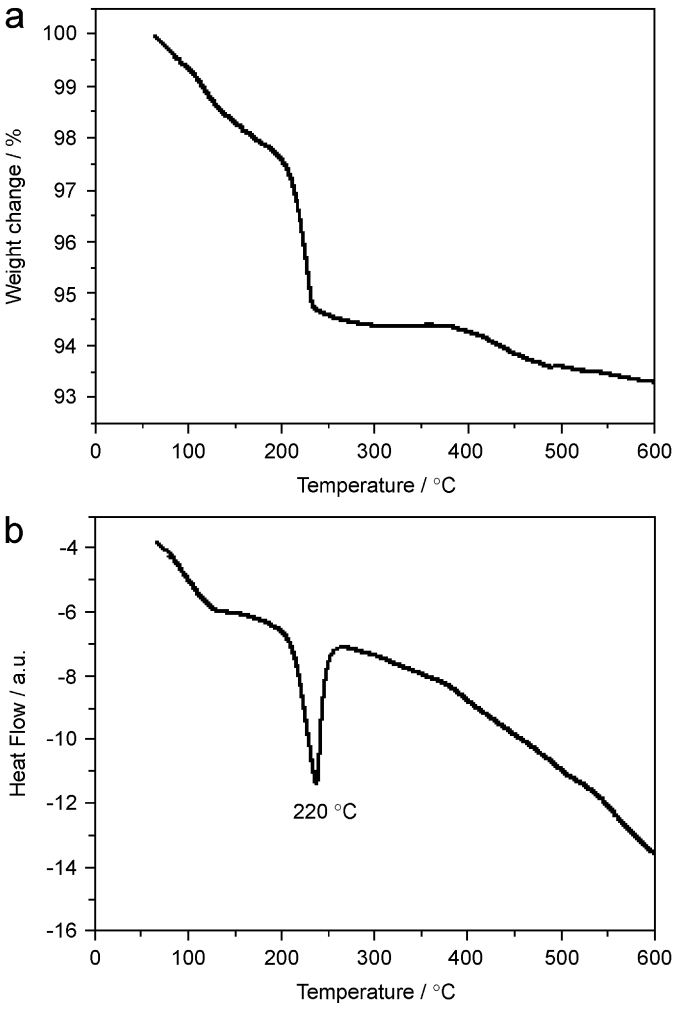

Fig. 2. TGA (a) and DTA (b) curves of the as-synthesized $TbPO_4$:Eu hydrate.

curve in the temperature range 60–140 °C. The second weight loss (5.5%) begins at about 150 °C; this corresponds to the dehydration of the hydrated hexagonal $TbPO_4$. Also, a corresponding well-defined endothermic peak is observed in DTA curve in the temperature range 150–300 °C with a sharp peak at 220 °C. The weight loss of 5.5% resulting from the dehydration means about 1 mol H_2O in the $TbPO_4 \cdot nH_2O$. It can be observed from XRD patterns that the sample annealed at 600 °C, which is dehydrated completely, still maintains the original crystal structure. This corresponds to the following equilibrium: $TbPO_4 H_2O_{(hexagonal)} \rightarrow TbPO_{4(hexagonal)} + H_2O$ [14,15]. Fig. 3 shows the SEM images of the as-synthesized and heat-treated samples, from which the uniform bundle-like morphology of $TbPO_4$:Eu is observed clearly (Fig. 3(a)). A magnified image (Fig. 3(c)) indicates that the bundle-like structure is actually composed of a self-assembly of the oriented nanowires with a diameter of about 40 nm and a length of 2–μm. These $TbPO_4$:Eu bundle-like structure are so stable that even at a high heat-treatment temperature, 600 °C, there is no evidence for any separation or change (Fig. 3(b)). Generally, controlled construction of nanosized units requires the assistance of copolymers or surfactants acting as direction functions during the synthesis [16]. However, it is surprising to observe ordered nanowire-based assemblies with bundle-like structure in the absence of copolymers and surfactants in our synthesis. Except for the rare earth orthophosphates [11], the formation of the

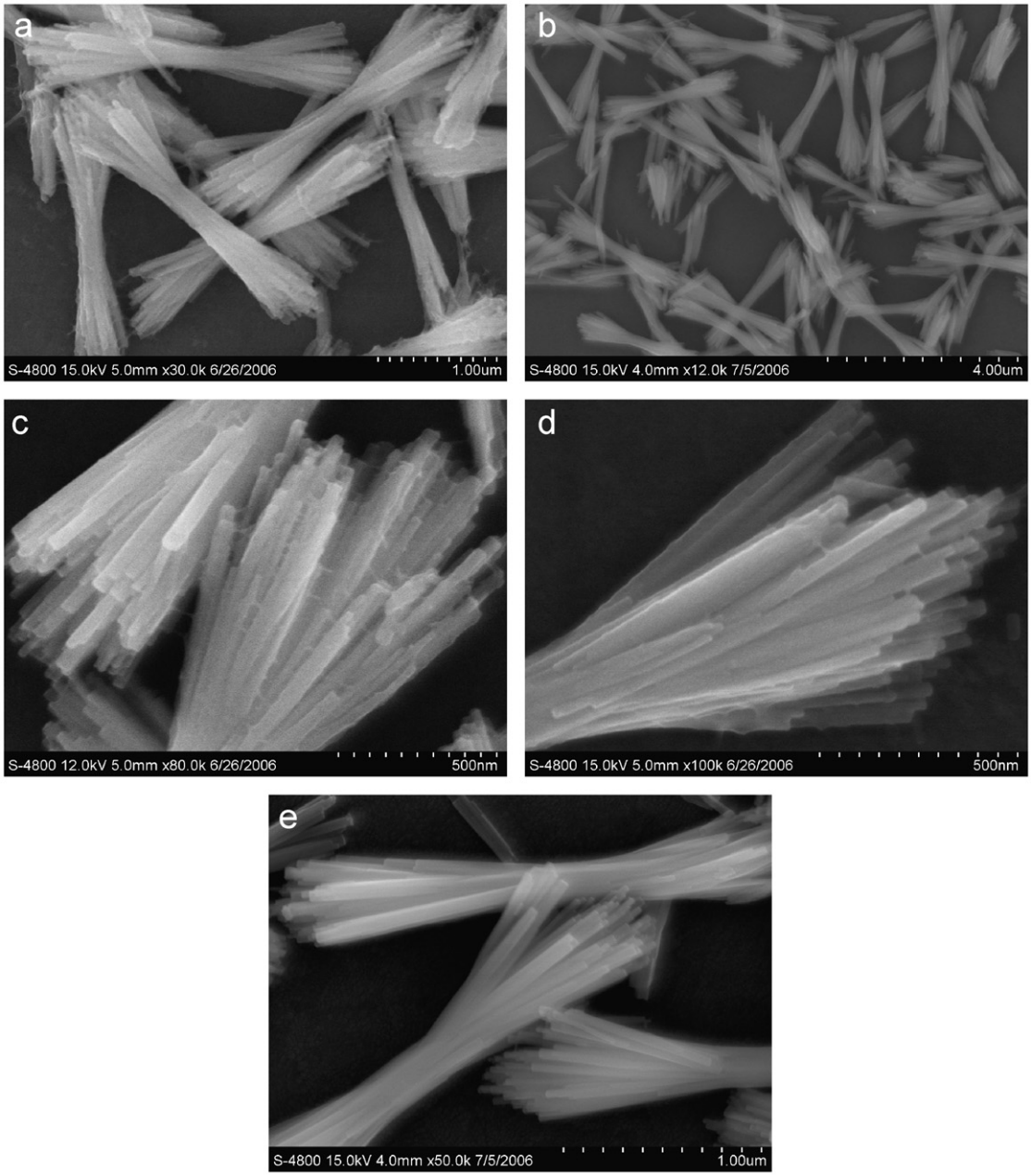

Fig. 3. SEM images of as-synthesized and heat-treated samples. (a) and (c): as-synthesized; (b) and (e): heat-treated at 600 °C; (d) heat-treated at 400 °C.

bundle-shaped structure made of nanorods/nanowires can also be observed for several systems, such as the growth of fluoroapatite in gelatin gels [17]. The exact growth mechanism is unknown, although some explanation was given in the literature based on the role of intrinsic electric field, which directs the growth of dipole crystals [18].

It is interesting to see that the nanowires building up bundle-like structure maintain their original size and shape in the heat-treatment process (Fig. 3(d)), even at a higher temperature (Fig. 3(e)). Also, it is worth noting that the heat-treatment plays an important role in the increase of crystallinity and the removal of impurities adsorbed at the surface. For the as-synthesized sample, ambiguous edges of nanowires and numerous surface adsorptions are observed (Fig. 3(c)). With the heat-treatment, the well-defined edge and the clear surface of nanowires can be seen due to the increase of crystallinity and the removal of adsorbed impurities (Fig. 3(e)). These adsorptions probably originate from the synthesis residues and byproducts. Furthermore, these adsorbed species at the surface might play an important role in inhibiting the growth of $TbPO_4$:Eu nanowires, since almost not any changes in the size and shape are observed with the increase of heat-treatment temperature.

Fig. 4 shows the emission spectra of $Tb_{1-x}PO_4:Eu_x$ ($x = 0,\ 0.005,\ 0.03$) under 355-nm excitation. In the undoped $TbPO_4$, the characteristic emissions of Tb^{3+} are observed, which originate from the transition between different f-electron states of Tb^{3+}, i.e., from the excited $^5D_4$ to the ground states $^7F_j (j = 6,\ 5,\ 4,\ 3)$ [12,19]. With the doping of Eu^{3+}, besides Tb^{3+} emission, we can also observe the characteristic emission of Eu^{3+} originating from the transition from the excited $^5D_0$ to the ground states ^7F_j [20], but the emission of Tb^{3+} decreases. With the increase of Eu^{3+} concentration, the luminescence of Tb^{3+} continues to decrease, and that of Eu^{3+} increases further. This indicates an efficient energy transfer from Tb^{3+} to Eu^{3+}. Also, such energy transfer behavior shows that the as-synthesized $TbPO_4$:Eu is not a mixture of $TbPO_4$ and $EuPO_4$, but a solid solution, in which Eu^{3+} has successfully incorporated into $TbPO_4$ lattice. Otherwise, the $Tb^{3+} \rightarrow Eu^{3+}$ energy transfer cannot occur in the separated phases. $Tb^{3+} \rightarrow Eu^{3+}$ energy transfer behavior is further confirmed by the luminescent dynamics of Tb^{3+}. Fig. 5 presents the fluorescent decay curves of $^5D_4$ of Tb^{3+} for $TbPO_4$ and $Tb_{0.995}PO_4:Eu_{0.005}$, respectively. It can be seen that, in the undoped $TbPO_4$ (Fig. 5(a)), the excited state $^5D_4$ of Tb^{3+} shows a fluorescent lifetime of about 0.55 ms. However, the doping of Eu^{3+} significantly modifies the fluorescent dynamics of Tb^{3+}. The $^5D_4$ state of Tb^{3+} shows a fast fluorescent decay, as a result, the lifetime deceases to about 0.13 ms (Fig. 5(b)). A schematic model is proposed for the energy transfer from Tb^{3+} to Eu^{3+}, as shown in Fig. 6. Since the $^5D_4$–^7F_j emission of Tb^{3+} is effectively overlapped with the $^7F_{0,\ 1}$–$^5D_{0,\ 1,\ 2}$ absorption of Eu^{3+} (see the dashed line with arrows), the energy transfer from Tb^{3+} to Eu^{3+} is very efficient [21].

With an increase of Eu^{3+} concentration in the Eu^{3+}-doped $TbPO_4$, the luminescence of Eu^{3+} is the competitive result of a pair of effects. On one hand, the increase of

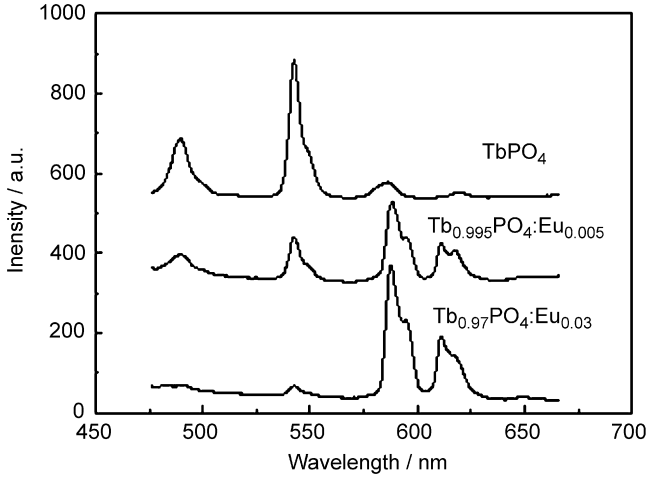

Fig. 4. Emission spectra of pure and Eu^{3+}-doped $TbPO_4$ under 355-nm excitation.

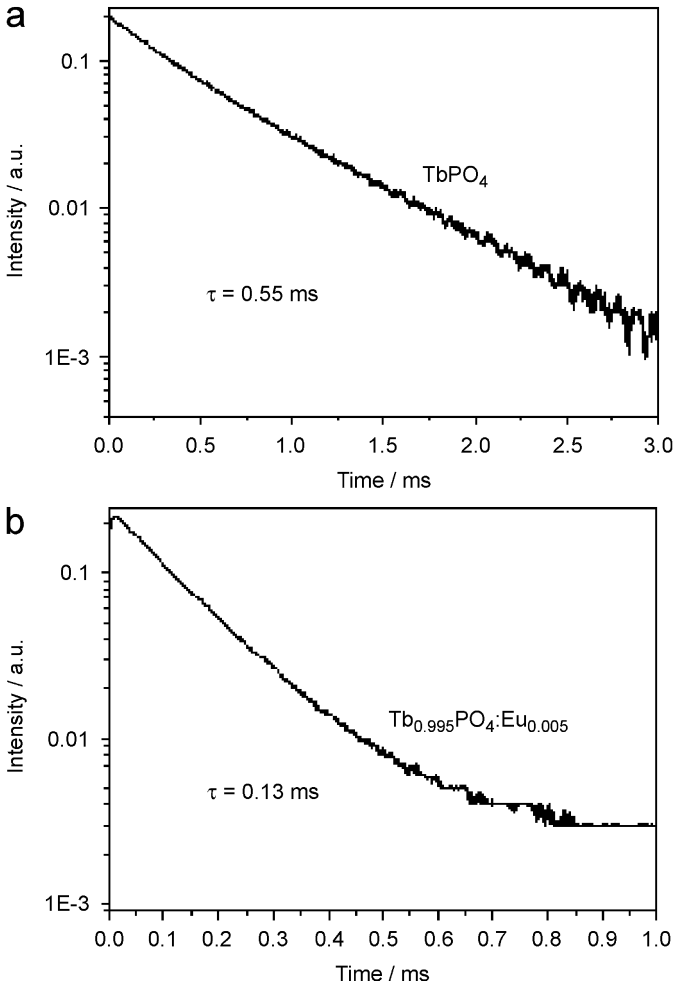

Fig. 5. Fluorescent decay curves of $^5D_4$ of Tb^{3+} in $TbPO_4$ doped with different Eu^{3+} concentrations.

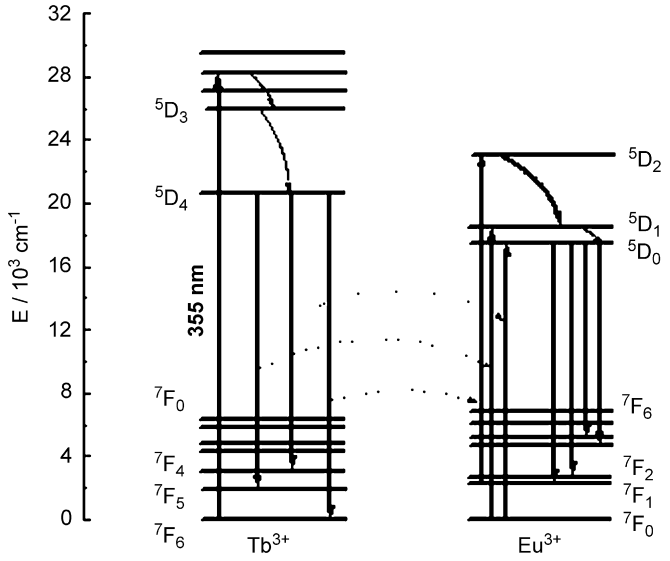

Fig. 6. A schematic model for the energy transfer from Tb^{3+} to Eu^{3+}.

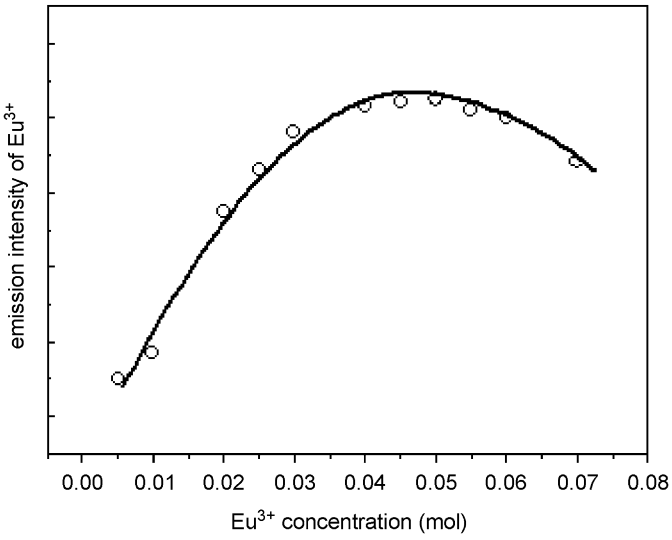

Fig. 8. Relative emission intensity of Eu^{3+} as a function of Eu^{3+} concentration.

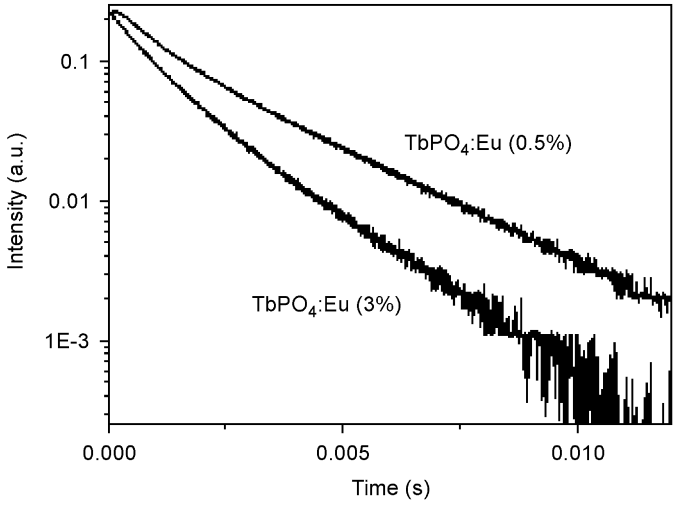

Fig. 7. Fluorescent decay curves of $^5D_0$ of Eu^{3+} in $TbPO_4$ doped with different Eu^{3+} concentrations.

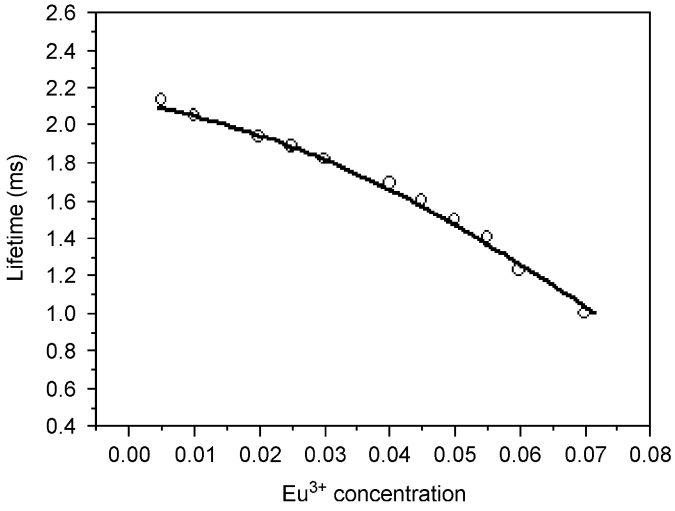

Fig. 9. Fluorescent lifetime of Eu^{3+} as a function of Eu^{3+} concentration.

Eu^{3+} concentration enhances the probability of energy transfer from Tb^{3+} to Eu^{3+}, which is evidenced by the decrease of the emission intensity and lifetime of the excited state of Tb^{3+}. On the other hand, the increase of Eu^{3+} concentration also increases the probability of nonradiative energy migration between Eu^{3+} ions up to quenching centers, where the excitation energy is lost nonradiatively [22]. This is confirmed by the fluorescent dynamics of Eu^{3+}, as shown in Fig. 7, from which a faster fluorescent decay of $^5D_0$ state of Eu^{3+} in $TbPO_4$:Eu (3% Eu^{3+}) is observed than that in $TbPO_4$:Eu (0.5% Eu^{3+}). To obtain an optimum dopant concentration, a series of samples doped with different Eu^{3+} concentrations are prepared, and their luminescence and the lifetime of $^5D_0$ of Eu^{3+} are measured and shown in Figs. 8 and 9. It can be seen that the luminescence of Eu^{3+} increase with Eu^{3+} concentration while Eu^{3+} concentration is lower than 5%, because more Eu^{3+} can obtain the energy transferred from Tb^{3+}. At this concentration range, $Tb^{3+} \rightarrow Eu^{3+}$ energy transfer is dominative to the luminescence of Eu^{3+}. However, while Eu^{3+} concentration is higher than 5%, the luminescence shows a decrease with the increase of Eu^{3+} concentration due to the concentration quenching effect. The lifetime of $^5D_0$ of Eu^{3+} always presents a decrease with increasing Eu^{3+} concentration due to the interaction between the neighboring Eu^{3+} up to a quenching center, as shown in Fig. 9. Especially for $TbPO_4$ doped with more than 5% mol Eu^{3+}, the fluorescent decay of Eu^{3+} shows a faster ratio.

Fig. 10 shows the effect of thermal treatment on the luminescence of Tb^{3+} and Eu^{3+} for the sample $TbPO_4$:Eu (0.5% Eu^{3+}). To prevent Tb^{3+} oxidation, annealing was carried out in N_2 atmosphere. It is noted that, with an increase of annealing temperature, the luminescence of Tb^{3+} decreases, but the luminescence of Eu^{3+} increases.

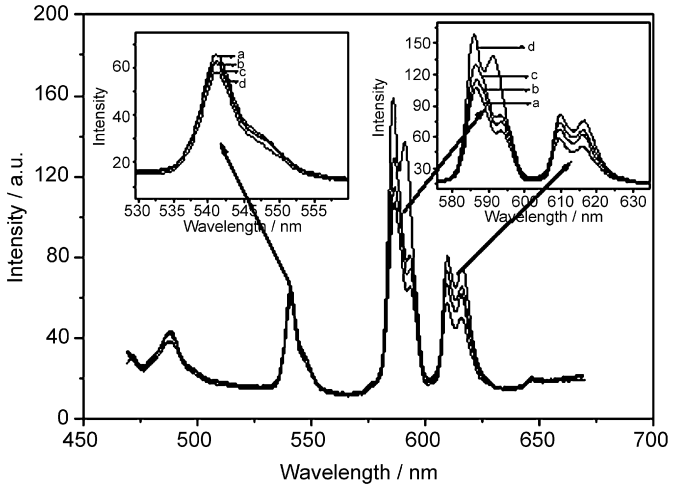

Fig. 10. Emission spectra of as-synthesized $TbPO_4$:Eu (0.5 %) and those heat-treated at various temperatures: (a) as-synthesized; (b) heated at 200 °C; (c) heated at 400 °C; (d) heated at 600 °C.

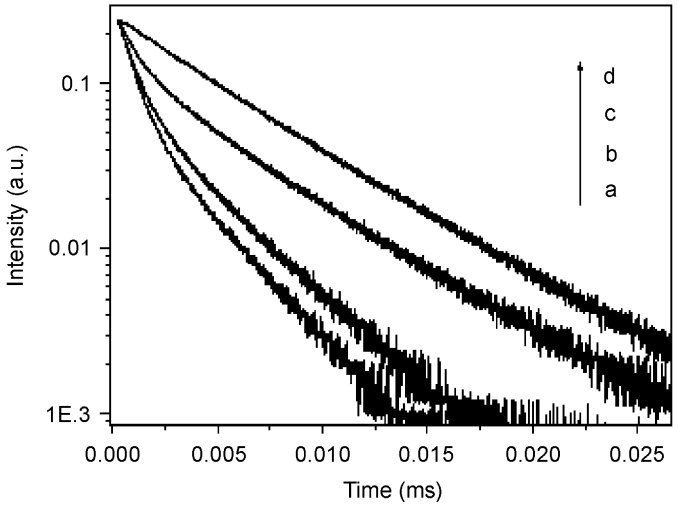

Fig. 11. Fluorescent decay curves of $^5D_4$ of Tb^{3+} for $TbPO_4$:Eu (0.5 %) as a function of heat-treatment temperature: (a) as-synthesized; (b) heated at 200 °C; (c) heated at 400 °C; (d) heated at 600 °C.

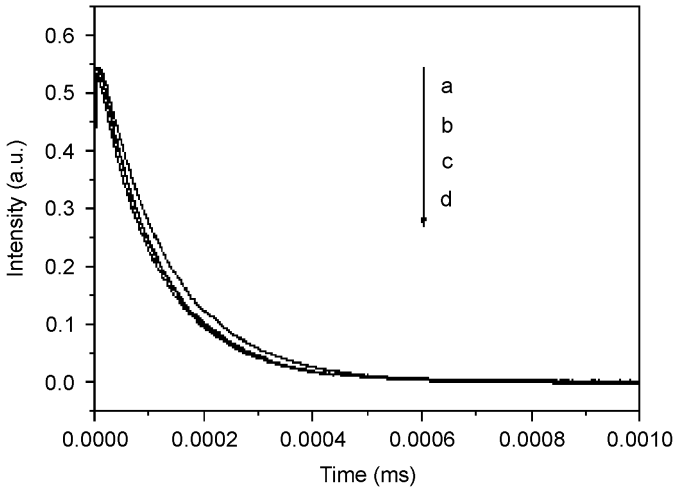

Fig. 12. Fluorescent decay curves of Eu^{3+} for $TbPO_4$:Eu (0.5 %) as a function of heat-treatment temperature: (a) as-synthesized; (b) heated at 200 °C; (c) heated at 400 °C; (d) heated at 600 °C.

This is probably because that $Tb^{3+} \rightarrow Eu^{3+}$ energy transfer becomes more efficient with the thermal treatment. But a careful observation finds that the decrease of Tb^{3+} luminescence is not equal to the increase of Eu^{3+} luminescence, i.e., the increase of Eu^{3+} luminescence is much more than the decrease of Tb^{3+} luminescence. This indicates that at least there is another factor that influences the luminescence of Tb^{3+} and Eu^{3+}. It is well known that surface always plays an important role in determining the luminescent properties, especially for the nanosized materials due to a large surface-to-volume ratio. In the nanosized $TbPO_4$:Eu, due to lower crystallinity and disordered environment around surface atoms, the Tb^{3+} ions at the surface are unable to fully coordinate to oxygen atoms. This inevitably leads to the existence of Tb^{3+} dangling bonds at the surface, which can arrest anion groups such as OH^- and NO_3^- [12,23]. Furthermore, the as-synthesized $TbPO_4$:Eu hydrates contain the structural water molecule. It is well known that these chemical species such as OH^- and H_2O possesses high vibration frequency ranging from 3000 to 4000 cm^{-1}, and always acts as efficient quenchers of luminescent lanthanide ions by multiphonon relaxation [12,23,24]. It is found that the $^5D_0$–$^7F_6$ energy gap for Eu^{3+} is smaller than the $^5D_4$–$^7F_0$ energy gap for Tb^{3+}, as shown in Fig. 6. This makes the nonradiative relaxation for Eu^{3+} by high-energy vibration of these chemical species much more probable than that for Tb^{3+}, which is evidenced by the fluorescent dynamics of $^5D_0$–$^7F_1$ of Eu^{3+} and $^5D_4$–$^7F_5$ of Tb^{3+} as a function of the heat-treatment temperature, as shown in Figs. 11 and 12, respectively. It can be seen that the fluorescent decay of Tb^{3+} shows only a little change, but a large change for Eu^{3+} is observed. In the as-synthesized $TbPO_4$:Eu^{3+} hydrate, the fluorescent decay of $^5D_0$ of Eu^{3+} significantly deviates from a single-exponential behavior due to the presence of structural water and the adsorption of impurity ions that act as the nonradiative relaxation channels to decrease the lifetime and emission efficiency of the excited state. With the increase of thermal treatment temperature, due to the disappearance of structural water and the removal of adsorbed impurity ions, the decay deviates much less from single-exponential behavior, and the emission efficiency increases gradually. Up to 600 °C, an almost single-exponential decay and significant increase of fluorescent time are observed.

4. Conclusions

Eu^{3+}-doped $TbPO_4$ ultralong nanowires have been successfully synthesized, which are orderly oriented to form the bundle-shaped structure. A thermal treatment up to 600 °C does not modify the size and shape of as-synthesized sample. Also, this thermal treatment process

removes the structural water of as-synthesized hydrates, but the crystal structure remains, i.e., $TbPO_4 H_2O_{(hexagonal)} \rightarrow TbPO_{4(hexagonal)} + H_2O$. Due to the energy overlap between Tb^{3+} and Eu^{3+}, an efficient energy transfer occurs from Tb^{3+} to Eu^{3+}. The increase of Eu^{3+} concentration leads to the increase of the energy transfer efficiency from Tb^{3+} to Eu^{3+}, but also enhances the probability of the interaction between neighboring Eu^{3+}, which results in the concentration quenching. The effect of the heat-treatment on the luminescent efficiency and lifetime of Tb^{3+} and Eu^{3+} is investigated. With the heat-treatment, the luminescence of Eu^{3+} presents an obvious increase, but almost no change for the luminescence of Tb^{3+}. The fluorescent dynamics of Eu^{3+} shows that the increase of luminescent efficiency of Eu^{3+} originates from the removal of structural water and adsorption ions, which act as the nonradiative relaxation channels of the excited state of Eu^{3+} by their high-energy vibration. In contrast, the $^5D_4$–$^7F_0$ energy gap for Tb^{3+} is larger than the $^5D_0$–$^7F_6$ energy gap for Eu^{3+}, as a result, structural water and adsorption ions show little effect on the luminescence of Tb^{3+}. The reported results on the energy transfer from Tb^{3+} to Eu^{3+} and the thermal treatment effects of photoluminescence of Tb^{3+} and Eu^{3+} can be well applied to other commonly used optical systems.

Acknowledgments

This work was supported by the National Natural Science Foundation of China (Grant Nos. 50502031, 50572102), and the Youth Fund of Jilin Province (Grant No. 20060522).

References

[1] T. Jüstel, H. Nikol, C. Ronda, Angew. Chem. Int. Ed. 41 (1998) 3084.
[2] G. Hebbink, J. Stouwdam, D. Reinhoudt, E. Beggel, Adv. Mater. 14 (2002) 1147.
[3] X. Duan, Y. Huang, Y. Cui, J. Wang, C. Lieber, Nature 409 (2001) 66.
[4] W.B. Bu, Z.L. Hua, H.R. Chen, J.L. Shi, J. Phys. Chem. B 109 (2005) 14461.
[5] X. Wang, Y.D. Li, Chem. Eur. J. 9 (2003) 5627.
[6] O. Lehmann, H. Meyssamy, K. Kompe, H. Schnablegger, M. Haase, J. Phys. Chem. B 107 (2003) 7449.
[7] S. Lucas, E. Champion, D. Bregiroux, D. Bernache-Assollant, F. Audubert, J. Solid State Chem. 177 (2004) 1302.
[8] W.B. Bu, H.R. Chen, Z.L. Hua, Z.C. Liu, W.M. Huang, L.X. Zhang, J.L. Shi, Appl. Phys. Lett. 85 (2004) 4307.
[9] C.J. Jia, L.D. Sun, F. Luo, X.C. Jiang, L.H. Wei, C.H. Yan, Appl. Phys. Lett. 84 (2004) 5305.
[10] W.H. Di, X.J. Wang, B.J. Chen, S.Z. Lu, X.G. Ren, Appl. Phys. Lett. 88 (2006) 011907.
[11] Y.P. Fang, A.W. Xu, A.M. Qin, R.J. Yu, Crys. Growth Des. 5 (2005) 1221.
[12] W.H. Di, X.J. Wang, B.J. Chen, S.Z. Lu, X.X. Zhao, J. Phys. Chem. B 109 (2005) 13154.
[13] K. Rajesh, P. Mukundan, P. Krishna Pillai, V.R. Nair, K.G.K. Warrier, Chem. Mater. 16 (2004) 2700.
[14] C.R. Patra, G. Alexandra, S. Patra, D.S. Jacob, A. Gedanken, A. Landau, Y. Gofer, New J. Chem. 29 (2005) 733.
[15] S. Lucas, E. Champion, D. Bernache-Assollant, G. Leroy, J. Solid State Chem. 177 (2004) 1312.
[16] A. Boal, F. Ilhan, J. Derouchey, T. Thurn-Albrecht, T. Russell, V. Rotello, Nature 404 (2000) 746.
[17] R. Kniep, S. Busch, Angew. Chem., Int. Ed. Engl. 35 (1996) 2624.
[18] L.Z. Zhang, J.C. Yu, A.W. Xu, L. Q, K.W. Kwong, S.H. Yu, J. Cryst. Growth 266 (2004) 545.
[19] W.F. van der weg, J.A. Popma Th, A.T. Vink, J. Appl. Phys. 57 (1985) 5450.
[20] X.C. Jiang, L.D. Sun, C.H. Yan, J. Phys. Chem. B 108 (2004) 3387.
[21] W. Chen, R. Sammynaiken, Y. Huang, J. Appl. Phys. 88 (2000) 1424.
[22] A. Huignard, T. Gacoin, J.P. Boilot, Chem. Mater. 12 (2000) 1090.
[23] K. Riwotzki, M. Haase, J. Phys. Chem. B 102 (1998) 1029.
[24] C. Jacinto, S.L. Oliveira, L.A.O. Nunes, T. Catunda, Appl. Phys. Lett. 86 (2005) 071911.